

Violation of the Cauchy-Schwarz Inequality in the Macroscopic Regime

A. M. Marino, V. Boyer, and P. D. Lett

*Joint Quantum Institute, National Institute of Standards and Technology,
and University of Maryland, Gaithersburg, Maryland 20899, USA*

(Dated: October 26, 2018)

We have observed a violation of the Cauchy-Schwarz inequality in the macroscopic regime by more than 8 standard deviations. The violation has been obtained while filtering out only the low frequency noise of the quantum-correlated beams that results from the technical noise of the laser used to generate them. We use bright intensity-difference squeezed beams produced by four-wave mixing as the source of the correlated fields. We also demonstrate that squeezing does not necessarily imply a violation of the Cauchy-Schwarz inequality.

PACS numbers: 42.50.Xa, 42.50.Dv, 42.65.Yj

The comparison between the predictions of quantum and classical theories has been a subject of study since the development of quantum mechanics. To that end, a number of different classical inequalities have been developed that provide an experimental discrimination between these theories [1, 2]. Experiments showing a violation of these classical inequalities have verified quantum theory. However, to date, most of these experiments have been carried out in the regime in which single particles are detected one at a time. It is thus interesting to study whether or not the quantum signature given by these tests is still present in the limit in which the system under study becomes macroscopic.

Among the inequalities that offer a test between quantum and classical theories is the Cauchy-Schwarz inequality (CSI) [1, 2]. The first observation of a violation of this inequality was obtained by Clauser using an atomic two-photon cascade system [3]. More recently, large violations using four-wave mixing have been obtained [4, 5], still in the photon-counting regime. For bright fields the natural approach for analyzing their quantum nature is through noise measurements. In this case the boundary between quantum and classical is taken to be the noise of a coherent state, or standard quantum limit (SQL), such that having a field with less noise than the SQL (squeezed light) is considered non-classical. However, the presence of squeezing does not provide a direct discrimination between quantum and classical theories since the SQL is a result of quantum theory [2].

The possibility of using a macroscopic quantum state to violate the CSI has been previously analyzed [6, 7, 8, 9]. To date, however, only a few experiments have probed this macroscopic regime. Recently anti-bunching of a small number of photons was observed in the continuous-variable regime [10]. In addition, a frequency analysis has been used to infer a violation of the CSI over limited frequency ranges [11].

In this Letter we present the first observation, to our knowledge, of a direct violation of the two-beam Cauchy-Schwarz inequality in the limit of a macroscopic quantum state. We show that the quantum-correlated fluctuations

between two different modes of the electromagnetic field are responsible for the violation of the CSI. In addition to having a bright coherent carrier, we work in the high gain regime in which the mean number of spontaneous correlated photons within the inverse of the bandwidth (correlation time) of the process is much larger than one. Thus photon counting is not an option and continuous variable detection schemes need to be used.

The CSI for the degree of second-order coherence, $g^{(2)}$, for two distinct fields, a and b , is of the form [12]

$$[g_{ab}^{(2)}(\tau)]^2 \leq g_{aa}^{(2)}(0)g_{bb}^{(2)}(0), \quad (1)$$

where $g^{(2)}$ is the normalized intensity correlation function. This inequality indicates that for a classical system the cross-correlation between two fields, $g_{ab}^{(2)}$, cannot be larger than the geometric mean of the zero-time auto-correlations, $g_{aa}^{(2)}$ and $g_{bb}^{(2)}$. According to quantum theory, however, it is possible to violate this inequality. In this case the correlation function is defined in terms of normally ordered operators

$$g_{ab}^{(2)}(\tau) = \frac{\langle \hat{a}^\dagger(t)\hat{b}^\dagger(t+\tau)\hat{b}(t+\tau)\hat{a}(t) \rangle}{\langle \hat{a}^\dagger(t)\hat{a}(t) \rangle \langle \hat{b}^\dagger(t)\hat{b}(t) \rangle}, \quad (2)$$

where \hat{a} and \hat{b} are the photon annihilation operators for the two fields. A violation of the CSI indicates the presence of non-classical correlations between the fields.

Most of the experiments to date have been done in the photon-counting regime, in which the separation between photon pairs is much larger than the correlation time between photons. This makes it possible to obtain a large cross-correlation while the zero time auto-correlation functions are in principle equal to 2, giving as a result a large violation of the CSI [12]. In contrast, in the large gain regime all of the correlation functions tend to the same value (they are equal or larger than one), making it harder to observe a violation of the CSI.

We use a seeded four-wave mixing (4WM) process in a double- Λ system in rubidium vapor, as described in [13, 14], as our source of bright correlated beams. Four-wave mixing is a parametric process, such that the initial and

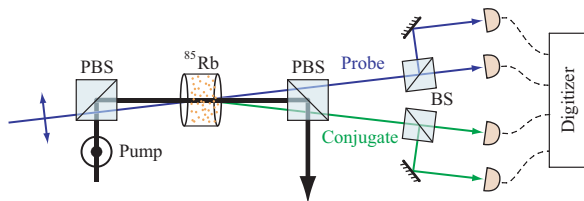


FIG. 1: (color online). Experimental setup. A 4WM process is used to generate quantum-correlated bright beams. PBS = polarizing beam splitter, BS = 50/50 beam splitter.

final states of the atomic system are the same. This leads to the emission of probe and conjugate photons in pairs and thus to intensity correlations between the two fields which are stronger than any correlations possible between classical optical fields.

The configuration and experimental parameters for the 4WM are the same as the ones described in Ref. [14]. A single Ti:Sapphire laser and an acousto-optic modulator are used to generate a bright pump and a weak probe which are resonant with a two-photon Raman transition between the $F = 2$ and $F = 3$ electronic ground states of ^{85}Rb . The pump laser is tuned 800 MHz to the blue of the D1 line at 795 nm while the probe is downshifted in frequency by 3 GHz. The two beams are then mixed at a small angle in a pure ^{85}Rb vapor cell, as shown in Fig. 1. In our double- Λ configuration, the 4WM converts two photons from the pump into one probe photon and one conjugate photon (upshifted by 3 GHz with respect to the pump). We have measured up to 8 dB of intensity-difference squeezing at 1 MHz with this method.

After the vapor cell we separate the probe and conjugate from the pump beam with a polarizer with $\approx 10^5 : 1$ extinction ratio for the pump. We then use beamsplitters to split the probe and conjugate, each into two beams of equal power, and detect the resulting four beams with separate photodiodes, as shown in Fig. 1. This setup directly measures the normally ordered correlation function defined in Eq. (2), as described in Ref. [2]. After each photodiode a bias-T is used to separate the DC part of the photocurrent, which is recorded and then used to normalize the correlation functions. The rest of the signal is amplified, digitized with a resolution of 9 bits, and recorded on a computer. The amplified time traces are sampled at a rate of 1 GS/s and 500 sets of traces, each with 10,000 points, are recorded. This setup allows us to simultaneously obtain all the information needed to calculate the correlation functions and the noise power spectra of the different beams.

The bright correlated beams that are obtained from the seeded 4WM process consist of a large coherent part plus quantum-correlated fluctuations. The large coherent part makes the $g^{(2)}$ functions tend to 1, the value for a coherent state, as its intensity increases. It is thus useful to separate the correlation functions into contributions

for the coherent part of the field and the fluctuations, that is $g_{ab}^{(2)} = 1 + \epsilon_{ab}$. Since the quantum correlations between the fields are in the fluctuations, we can rewrite the CSI in terms of the fluctuation terms such that it takes the form

$$\epsilon_{ab} \leq \frac{\epsilon_{aa} + \epsilon_{bb}}{2}, \quad (3)$$

where we have kept only terms to first order in ϵ . We define a violation factor

$$V \equiv \frac{\epsilon_{aa} + \epsilon_{bb}}{2\epsilon_{ab}} \quad (4)$$

such that $V < 1$ indicates a violation of the CSI.

In the ideal case, the 4WM process can be described by the two-photon squeeze operator $\hat{S}_{ab} = \exp(s\hat{a}\hat{b} - s\hat{a}^\dagger\hat{b}^\dagger)$, where s is the squeezing parameter ($s > 0$). The bright quantum-correlated beams are obtained by applying this operator to an input coherent state, $|\alpha\rangle$, for the probe and the vacuum for the conjugate. In the limit in which the number of photons in the probe seed is much larger than one ($|\alpha| \gg 1$) V takes the form

$$V = 1 - \frac{1}{2G}, \quad (5)$$

where $G = \cosh^2 s$ is the gain of the process and we have taken the single frequency approximation for each beam. For an ideal seeded 4WM process V is always less than one, so that a violation of the CSI should always be obtained. In general, however, the presence of squeezing does not guaranty a violation of the CSI. As Eq. (5) shows, the amount of violation is inversely proportional to the gain. This is in contrast to the amount of intensity-difference squeezing that is expected from a seeded 4WM process, for which the noise scales as $1/(2G - 1)$. Thus, a large amount of squeezing does not imply a large violation of the CSI, as has been pointed out in Ref. [15].

A typical set of correlation functions that shows a violation of the CSI is shown in Fig. 2. Here the horizontal dashed line indicates the mean value of the zero-time auto-correlation functions of the fluctuations for the probe and the conjugate, such that a cross-correlation larger than this level indicates a violation of the CSI. A violation of the CSI can clearly be seen in the inset of Fig. 2. In obtaining these correlation functions we have only filtered out the low frequency technical noise below 500 kHz. The bandwidth of the detection system (> 40 MHz) is larger than the bandwidth of the quantum correlations.

The uncertainties indicated in Fig. 2 are obtained by directly calculating the correlation functions and obtaining the standard deviation over the 500 sets of traces. These uncertainties are not statistically independent since the probe and conjugate contain classical fluctuations that are strongly correlated as a result of slow intensity fluctuations of the pump and probe seed beams

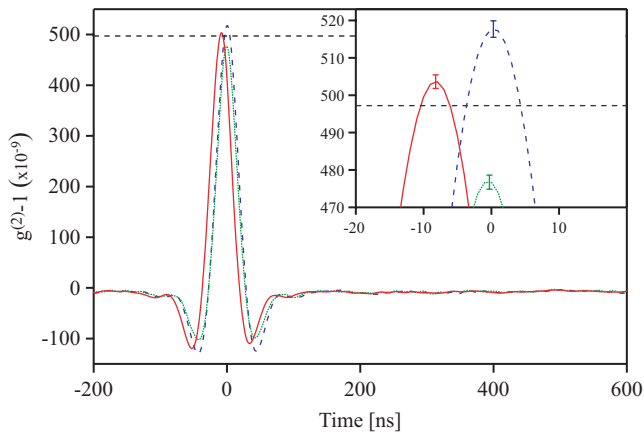


FIG. 2: (color online). Correlation functions of the fluctuations for the probe (dotted), conjugate (dashed), and cross $g^{(2)}$ (solid). The inset shows an expanded view of the peaks of the correlation functions. The horizontal dashed line shows the mean value of the zero time auto-correlation functions for the probe and the conjugate. The indicated uncertainties are discussed in the text.

between data sets. This leads to a violation of the CSI that is more significant than what can be inferred from the inset. An accurate measure of the uncertainty of V is obtained by calculating V for each set of traces and using these results to derive the standard deviation of V over the 500 sets. For the results shown in Fig. 2 the gain of the process is around 10 and $V = 0.987 \pm 1.4 \times 10^{-3}$, giving a violation of the CSI by more than 8 standard deviations.

The cross-correlation function shows a delay in the arrival time between probe and conjugate fluctuations; for the case shown in Fig. 2 the delay is around 8 ns. The delay results from the combination of 4WM in the double- Λ system and propagation through the vapor cell [16, 17]. An important property of the double- Λ system is that the relative delay between probe and conjugate for fluctuations of different frequencies is almost fixed. Such a fixed delay only causes the cross-correlation to be shifted in time and will not have an effect on V . In contrast, any large spread in the delay between different frequencies (dispersion) would make the cross-correlation peak wider and reduce its maximum value, degrading the amount of violation. The dips on the correlation functions are due to an offset of the carrier frequency with respect to the gain peak of the process. These effects will be examined in detail elsewhere.

One of the difficulties in obtaining a violation of the CSI is that any source of excess uncorrelated noise will decrease the violation. In order to see why this is the case, we need to consider the noise power spectra of the different beams. We can rewrite the CSI in terms of the noise power spectra for the probe (S_p), conjugate (S_c),

and intensity-difference (S_{diff}) such that

$$\int d\Omega \left(\frac{S_{\text{diff}}(\Omega)}{\langle \hat{n}_p \rangle + \langle \hat{n}_c \rangle} - 1 \right) \geq \frac{\langle \hat{n}_p \rangle - \langle \hat{n}_c \rangle}{\langle \hat{n}_p \rangle + \langle \hat{n}_c \rangle} \int d\Omega \left[\left(\frac{S_p(\Omega)}{\langle \hat{n}_p \rangle} - 1 \right) - \left(\frac{S_c(\Omega)}{\langle \hat{n}_c \rangle} - 1 \right) \right]. \quad (6)$$

The terms in parenthesis represent the excess noise (or noise reduction) with respect to the corresponding SQL. For the ideal seeded 4WM process the normalized noise power spectra for the probe and the conjugate are equal, so that the term in square brackets is zero, and $\langle \hat{n}_p \rangle > \langle \hat{n}_c \rangle$. The presence of squeezing in the intensity difference can make the integral on the left hand side negative, leading to a violation of the CSI. Excess noise can have an impact on the violation in two different ways. The presence of excess uncorrelated noise on either beam can lead the intensity-difference noise to go above the SQL for some frequency ranges such that the integral on the left hand side can become positive. In addition, excess noise on the conjugate can make the right hand side of the inequality negative enough (given that $\langle \hat{n}_p \rangle > \langle \hat{n}_c \rangle$) so that even if squeezing is present a violation might not be obtained.

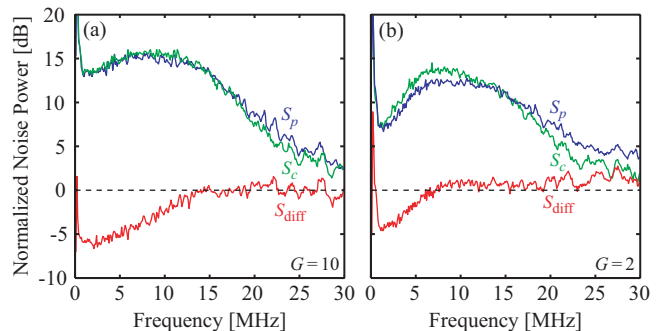


FIG. 3: (color online). Normalized noise power spectra for the probe (S_p), conjugate (S_c), and intensity-difference (S_{diff}) for a gain of (a) 10 and (b) 2. All the spectra are normalized to their respective SQL, represented by the dashed line.

For the results shown in Fig. 2, the corresponding normalized noise power spectra are shown in Fig. 3(a). All the noise power spectra are calculated by taking the FFT of the time traces and averaging over the 500 sets. The SQL for the probe and conjugates is calculated by taking the difference of the corresponding photocurrents while the one for the intensity-difference noise is given by the sum of the SQLs for the probe and conjugate. As is expected for a 4WM process both the probe and the conjugate have excess noise with respect to the SQL and their spectra are almost the same. The measured intensity-difference squeezing has a bandwidth of 15 MHz, consistent with the gain bandwidth of the 4WM process [17], with a maximum squeezing of 6 dB. For this case the system acts almost as an ideal 4WM medium which makes

it possible to observe a violation of the CSI. The amount of squeezing that is measured is limited by a total detection efficiency, including optical path transmission and photodiode efficiencies, of $(80 \pm 3)\%$. We have verified that $g^{(2)}$ is not affected by loss so that any source of loss will not have an impact on the violation of the CSI.

When the gain of the process is reduced to 2, we find a situation in which the noise power spectra of the probe and the conjugate are noticeably different, as shown in Fig. 3(b). This difference in noise leads to a reduction of the intensity-difference squeezing bandwidth from 15 MHz to 7 MHz and a small amount of excess noise at higher frequencies. For this particular case we find that the small amount of excess noise is enough to prevent a violation of the CSI, such that $V = 1.075 \pm 3.3 \times 10^{-3}$, even though there is more than 4 dB of squeezing at low frequencies.

The relative delay between the probe and the conjugate (8 ns for $G = 10$ and 13 ns for $G = 2$) has been compensated when calculating the intensity-difference noise power spectra shown in Fig. 3. This makes it possible to see the real squeezing bandwidth that results from the 4WM process in Fig. 3(a). While the relative delay has no effect on the violation of the CSI, it introduces a frequency dependent phase shift such that the intensity-difference noise power spectrum oscillates between intensity-difference and intensity-sum noise levels [18].

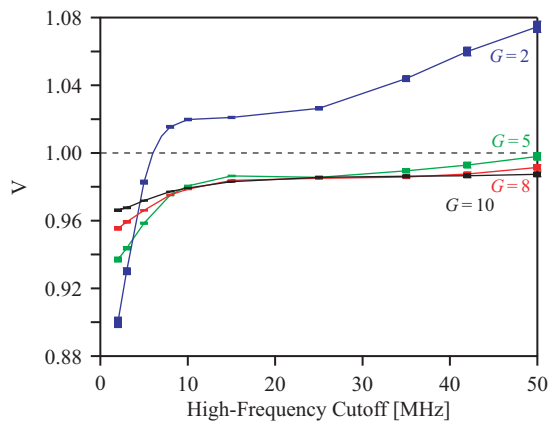


FIG. 4: (color online). Effect of frequency filtering on the violation of the CSI. Violation parameter (V) as a function of high-frequency cutoff for $G = 2$, $G = 5$, $G = 8$, and $G = 10$. $V < 1$ indicates a violation of the CSI. The size of the squares represent the statistical uncertainties.

The effect of the excess noise can be further analyzed by filtering out the high frequencies, where most of the uncorrelated excess noise is present. The filtering is done on the digitized traces by applying a 10th order Butterworth bandpass filter with a low-frequency cutoff of 500 kHz that filters out the technical noise of the laser and a variable high-frequency cutoff. We have done this

analysis for a number of different gains, as shown in Fig. 4. The gain is changed by modifying the temperature of the cell and thus the atomic number density.

If we look at the lowest high-frequency cutoff points in Fig. 4, we see that the violation follows the trend given by Eq. (5) for an ideal 4WM process, that is, the violation gets better with smaller gains. However, once we increase the high-frequency cutoff, V starts to degrade, with lower gains degrading faster. Increasing the high-frequency cutoff takes into account higher frequencies of the noise power spectrum that correspond to different regions of the gain profile. This leads to competition with other processes, such as Raman gain on the conjugate, that add excess noise. Except for the case $G = 2$ a violation of the CSI is obtained for the different gains shown in Fig. 4 when only the low frequency technical noise of the laser is filtered. Even for the case in which the system contains excess uncorrelated noise, a violation of the CSI can be recovered with enough filtering, as shown for the case of $G = 2$. This approaches a spectral analysis of the noise, as is regularly done when measuring bright beams.

If we compare the case of $G = 2$ in Fig. 3 and Fig. 4 we find that the violation is lost at a high-frequency cutoff around 6 MHz while the squeezing is present over a larger frequency range than the filtering bandwidth used to calculate V , up to around 7 MHz, once the relative delay between probe and conjugate has been compensated. This gives a region in which squeezing is present but not a violation of the CSI. The amount of excess noise on the conjugate is enough to destroy the violation but not the squeezing.

In conclusion, we have observed a violation of the CSI in the macroscopic regime. The necessary information to observe the violation is contained in the quantum-correlated fluctuations of the field. We have shown that the presence of excess uncorrelated noise can prevent the observation of a violation of the CSI. The ability to obtain a violation of the CSI shows that the 4WM process used here provides a low-noise source of quantum correlated bright beams over a large frequency range. Finally, we have shown that the presence of squeezing does not necessarily imply a violation of the CSI.

-
- [1] R. Loudon, Rep. Prog. Phys. **43**, 913 (1980).
 - [2] M. D. Reid and D. F. Walls, Phys. Rev. A **34**, 1260 (1986).
 - [3] J. F. Clauser, Phys. Rev. D **9**, 853 (1974).
 - [4] P. Kolchin et al., Phys. Rev. Lett. **97**, 113602 (2006).
 - [5] J. K. Thompson et al., Science **313**, 74 (2006).
 - [6] K. J. McNeil and C. W. Gardiner, Phys. Rev. A **28**, 1560 (1983).
 - [7] C. C. Gerry and R. Grobe, Phys. Rev. A **51**, 1698 (1995).
 - [8] N. B. An and T. M. Duc, J. Opt. B **4**, 289 (2002).

- [9] M. K. Olsen, L. I. Plimak, and A. Z. Khoury, *Opt. Commun.* **215**, 101 (2003).
- [10] N. B. Grosse et al., *Phys. Rev. Lett.* **98**, 153603 (2007).
- [11] Y. Q. Li et al., *J. Opt. B* **2**, 292 (2000).
- [12] R. Loudon, *The Quantum Theory of Light* (Oxford Academic Press, Oxford, 2000).
- [13] C. F. McCormick et al., *Opt. Lett.* **32**, 178 (2007).
- [14] C. F. McCormick et al., arXiv:quant-ph/0703111 (2007).
- [15] H. J. Carmichael et al., *Phys. Rev. Lett.* **85**, 1855 (2000).
- [16] C. H. van der Wal et al., *Science* **301**, 196 (2003).
- [17] V. Boyer et al., *Phys. Rev. Lett.* **99**, 143601 (2007).
- [18] S. Machida and Y. Yamamoto, *Opt. Lett.* **14**, 1045 (1989).